Environmental Science & Technology

pubs.acs.org/est

Article

Reduction of Nonvolatile Particulate Matter Emissions of a Commercial Turbofan Engine at the Ground Level from the Use of a Sustainable Aviation Fuel Blend

Lukas Durdina,* Benjamin T. Brem,* Miriam Elser, David Schönenberger, Frithjof Siegerist, and Julien G. Anet

Cite This: *Environ. Sci. Technol.* 2021, 55, 14576−14585

Read Online

ACCESS | Metrics & More | Article Recommendations | Supporting Information

ABSTRACT: Nonvolatile particulate matter (nvPM) emissions from aircraft turbine engines deteriorate air quality and contribute to climate change. These emissions can be reduced using sustainable aviation fuels (SAFs). Here, we investigate the effects of a 32% SAF blend with fossil fuel on particle size distributions and nvPM emission indices of a widely used turbofan engine. The experiments were conducted in a test cell using a standardized sampling and measurement system. The geometric mean diameter (GMD) increased with thrust from ∼8 nm at idle to ∼40 nm at take-off, and the geometric standard deviation (GSD) was in the range of 1.74−2.01. The SAF blend reduced the GMD and GSD at each test point. The nvPM emission indices were reduced most markedly at idle by 70% in terms of nvPM mass and 60% in terms of nvPM number. The relative reduction of nvPM emissions decreased with the increasing thrust. The SAF blend reduced the nvPM emissions from the standardized landing and take-off cycle by 20% in terms of nvPM mass and 25% in terms of nvPM number. This work will help develop standardized models of fuel composition effects on nvPM emissions and evaluate the impacts of SAF on air quality and climate.

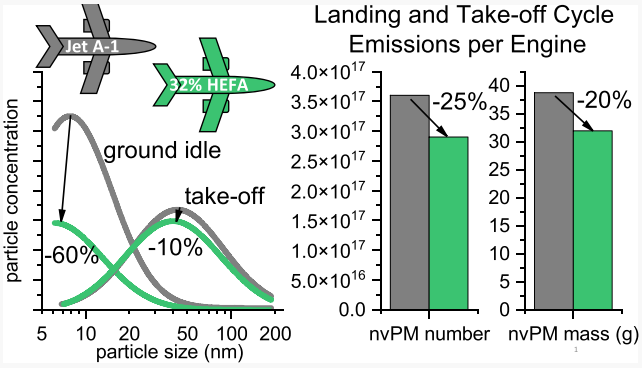

KEYWORDS: *aviation emissions, sustainable aviation fuel, particulate matter, black carbon, air pollution*

INTRODUCTION

The airline industry has pursued sustainable aviation fuels (SAFs) as one of the most promising measures to reduce aviation's adverse effects on the environment.[1] Currently, up to 50% of synthetic components made using various production pathways may be blended with conventional jet fuel.[2] Such drop-in blends fulfill the standard specification for aviation turbine fuels and can be readily used in today's aircraft without changes to operability and performance.[3] SAF blends reduce the carbon footprint of the fuel.[4] Due to their origin and refining, pure SAFs are virtually free of sulfur and aromatic hydrocarbons.[2] Thus, SAF blends directly reduce volatile and nonvolatile particulate matter (nvPM) emissions.[5−14]

With the prospect of increasing commercial use of SAFs, there is a growing interest in their PM emissions reduction potential at the ground level and cruising altitudes. In chase studies at cruising altitudes, SAF blends reduced nvPM mass and number emissions directly behind the aircraft by 50−97% compared to conventional Jet A-1 fuel.[10,13,15,16] Engine emission tests at the ground (on-wing and in a test cell) have shown PM emissions reductions of over 90%, depending on the blend ratio, engine technology, and power setting.[5−9,11,12,14,16] The nvPM emissions reduction is proportional to the decrease in soot precursors in the fuel.[17] The fuel composition effects on gas turbine nvPM emissions are correlated with total aromatics, naphthalenes, and the fuel hydrogen content. Especially, the fuel hydrogen content (% mass) has been used as a key variable in investigations of soot formation in gas turbine combustors since several decades.[18−20] The hydrogen content accounts for the differences in the degree of saturation of the aromatics (fewer ring structures in the fuel correspond to a lower number of hydrogen atoms). Several recent studies have found strong correlations of nvPM and total PM emissions with fuel hydrogen content.[6,11,21−23] The fuel composition effects on nvPM depend on the engine power setting. The highest reductions have been observed at a

Received: July 16, 2021
Revised: October 1, 2021
Accepted: October 4, 2021
Published: October 18, 2021

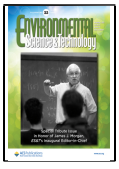

https://doi.org/10.1021/acs.est.1c04744
Environ. Sci. Technol. 2021, 55, 14576−14585

low engine power (idle and taxi), which has potential benefits for local air quality and health effects using SAFs.[8,11,16,21,24]

As the local air quality impacts of aviation's ultrafine PM emissions have become a growing concern, the International Civil Aviation Organization's Committee on Aviation Environmental Protection (ICAO CAEP) initiated a regulatory standard for nvPM emissions.[8,25−29] All in-production engines with rated thrust F_{oo} greater than 26.7 kN have to comply with the limit for the maximum nvPM mass concentration in the exhaust (CAEP/10 nvPM standard) and the limits for the nvPM mass and nvPM number emitted during the standard landing and take-off (LTO) cycle normalized by F_{oo} (CAEP/11 nvPM standard).[26,28,30] Although the nvPM certification requirement is in force, there are ongoing efforts to improve the measurement methodology and address uncertainty and variability sources. For example, the EU-funded projects AVIATOR and RAPTOR aim to quantify measurement uncertainties and variability due to instruments' calibration drift, particle losses in the sampling systems, ambient conditions, and fuel composition.[31,32] Despite numerous studies performed with SAFs, there is limited data acquired with standardized nvPM sampling and measurement systems for large commercial turbofan engines. Such data are necessary to develop a robust fuel composition effect model for nvPM certification and predict the impacts on local air quality. Most previous studies of fuel effects on aircraft engine PM emissions used sampling and measurement methodologies not compliant with the ICAO nvPM standard.[5,9−11,16,33] Large-scale engine testing is costly, and modern engine technologies are rarely accessible. Thus, many previous fuel effect studies were conducted on older technology engines, auxiliary power units (APUs), and laboratory combustors, which may not represent the current commercial fleet.[6,7,13,14,23,34,35]

Here, we investigate the effects of a blend of Jet A-1 with 32% of synthetic paraffinic kerosene from hydrotreated esters and fatty acids (HEFA-SPK) on particle size distributions and emission indices of nvPM mass (EI_{mass}) and nvPM number (EI_{num}) of the widely used CFM56-7B engine (Boeing 737 family). The engine exhaust was sampled and measured using the Swiss Mobile Aircraft Engine Emissions Measurement System (SMARTEMIS), one of the three reference sampling and measurement systems for nvPM.[25,26] The work was conducted during the EMPAIREX 1 campaign (Emissions of Particulate and gaseous pollutants in AIRcraft engineEXhaust), and it extends the work of Brem et al.[21] to thrust levels below 30% and different fuels with lower levels of total aromatics.

MATERIALS AND METHODS

Engine Emission Tests. Engine emission tests were performed on a CFM56-7B26 engine (Boeing 737NG series aircraft) in a test cell at SR Technics, Zurich Airport. The engine passed all performance tests for operations on commercial aircraft before and after the campaign. The engine was operated on a decreasing power curve from take-off to idle. The engine test points were set using the combustor inlet temperature T_3 in compliance with the ICAO emissions certification procedures.[30] The test points chosen were based on a correlation between engine thrust and T_3 at the sea level determined from a calibrated engine performance model for this engine type.[36] The test matrix contained seven test points: ground idle (~3%), 7, 30, 50, 65, 85, and 100% F_{oo} (F_{oo} = 117 kN). The duration of each test point was from 5 up to 90 min to accommodate various experiments performed during the campaign.[24,37]

Fuel Properties. The specifications of the fuels used are shown in Table 1. The neat Jet A-1 fuel was a standard batch

Table 1. Fuel Properties

property	ASTM method	unit	Jet A-1	32% HEFA-SPK blend
aromatics	D1319	vol %	18.1	11.3
naphthalene	D1840	vol %	0.79	0.53
hydrogen (NMR)	D7171 equivalent	mass %	13.57	14.05
hydrogen (CHN)	D5291	mass %	13.68	14.25
H/C ratio (NMR)			1.88	1.95
smoke point	D1322	mm	22	24
viscosity at −20 °C	D445	mm^2/s	3.41	3.68
specific energy	D3338	MJ/kg	43.3	43.6
density at 15 °C	D4052	kg/m^3	795.4	781.8
sulfur	D5453	ppm	490	350

used at Zurich Airport. The 32% HEFA-SPK blend was obtained by blending the residual Jet A-1 in the test cell fuel tank with 32.6 tons of a 44.4% blend of HEFA-SPK SAF supplied by SkyNRG. The neat HEFA-SPK was produced by AltAir Fuels (Paramount, CA; now part of World Energy) from used cooking oil. The neat SAF was shipped to Europe and blended with locally stored fossil jet fuel prior to delivery to SR Technics. The blend was certified to the ASTM D7566 standard for jet fuels containing synthesized hydrocarbons.[2] The data for aromatics, naphthalene, hydrogen content, and density are averages calculated from 14 samples (10 samples for Jet A-1 and 4 for the 32% HEFA blend). The remaining parameters are based on one fuel sample of Jet A-1 and two samples of the 32% HEFA blend. The analysis was performed by a certified laboratory (Intertek AG, Switzerland). Additionally, the hydrogen mass content was determined in-house by nuclear magnetic resonance (NMR) using a method equivalent to ASTM D7171.[38] The NMR-determined hydrogen content was used in our analysis. For comparison with previous studies, we list the hydrogen mass content determined by Intertek using the less accurate and precise method ASTM D5291 for determining carbon, hydrogen, and nitrogen content (CHN).[39]

Exhaust Sampling and Measurement. The exhaust sample was extracted <1 m downstream of the engine exit plane using a single-orifice probe with an inner diameter (ID) of 8 mm made of an Inconel 600 alloy. The probe sampling position was checked by carbon balance (air−fuel ratio of the exhaust sample agreed with the engine air−fuel ratio within 10% at all test points above idle). The extracted exhaust sample was transported via a trace-heated (160 °C) and insulated 5 m long stainless steel tube with 8 mm ID to a flow splitter and diluter assembly (diluter box). At the diluter box inlet, the sample was split into the pressure control line (diluter sample pressure control), the nvPM transfer section, and the raw gas line. The raw gas line (160 °C, length 25 m, 6 mm ID, flow rate ~18 slpm, carbon-filled poly(tetrafluoroethylene) (cPTFE)) transported the raw exhaust sample to the gas and smoke analysis system (CO_2, CO, NO_x, SO_2, HC, and smoke number). In the diluter box, a Dekati DI-1000 ejector diluter

https://doi.org/10.1021/acs.est.1c04744
Environ. Sci. Technol. 2021, 55, 14576−14585

diluted the exhaust sample with dry synthetic air by a factor of 8−11. The diluted sample was drawn through a trace-heated line (60 °C, length 24.2 m, 8 mm ID, flow rate 23 slpm, cPTFE) to the PM measurement rack. In the PM rack, the sample passed through a sharp cut cyclone (1 μm aerodynamic diameter cutoff) and was split to various aerosol instruments and a make-up flow line with a CO_2 analyzer (model 410i, Thermo Scientific). The nvPM number concentration (cutoff size d_{50} = 10 nm) was measured using an AVL Particle Counter Advanced (APC, AVL) and the nvPM mass concentration was measured using an AVL Micro Soot Sensor (MSS, AVL). The MSS is a real-time photoacoustic black carbon (BC) mass instrument.[40] BC mass, which is used as a surrogate for nvPM mass in the regulatory standard, is calibrated to the elemental carbon (EC) mass of diffusion flame soot.[29] The mass absorption cross section (MAC) of the calibration aerosol used by the manufacturer AVL has been found to agree with the MAC of aircraft gas turbine soot within 5%.[41] Diffusion flame soot calibration of the MSS has provided excellent agreement with EC mass at various operating conditions of aircraft turbine engines using fossil and synthetic fuels.[37,42] The particle size distributions were measured using a fast Scanning Mobility Particle Sizer (SMPS, model 3938, TSI Inc.) operating in a high flow mode (1.5 lpm nominal aerosol flow), sheath-to-aerosol flow ratio of 12, and with 30 s scan time. Additional aerosol instruments were used to characterize effective density, chemical and optical properties, and toxicity.[24,37]

Data Reduction. The emissions and engine data were averaged over 3−60 min during stable engine operation. The averaging periods followed a stabilization period of 1−3 min at each test point. Although 60 s averages are sufficient for the calculation of nvPM EIs (1 Hz sampling rate), the long averaging periods provided better statistics of the SMPS data.

The averaged data were filtered by ambient temperature to evaluate the fuel effects on nvPM emissions as accurately as possible. As described above, the engine test points were set using the combustor inlet temperature T_3. At a constant T_3, nvPM emissions can vary markedly with changes in ambient temperature mainly due to the effects of varying combustor inlet pressures.[26] If emission tests with different fuels are performed at different ambient conditions, the fuel composition effects could be impossible to evaluate, especially at test points where the nvPM emission characteristics vary significantly with small changes in engine operating conditions. The tests with Jet A-1 were performed at ambient temperatures between 2 and 17 °C and the SAF blend tests between 6.5 and 12 °C. We used only data obtained with both fuels in the ambient temperature range of 7.5−12 °C. The nvPM EIs for all ambient conditions can be found in the Supporting Information (SI).

Particle Loss Correction and Size Distributions. All results are reported at the engine exit plane, corrected for thermophoretic loss independent of the particle size and size-dependent particle loss in the sampling and measurement system. The thermophoretic loss due to a temperature gradient between the exhaust gas and the sampling line wall was calculated from the measured exhaust gas temperature and the sample line temperature.[35] The correction factor k_{thermo} ranged from 1.16 to 1.29. The size-dependent particle losses in the sampling and measurement system were calculated using the particle size distributions (PSDs) measured with the SMPS and modeled penetration functions. The penetration functions were modeled using the system loss tool of the SAE Aerospace Recommended Practice (ARP) 6481.[43] The penetration functions include the sampling system sections from the probe inlet to the instrument inlets. The nvPM number instrument has additional losses in the volatile particle remover (VPR; catalytic stripper and a secondary dilution system) and due to the CPC cutoff (10 nm), which are accounted for in the penetration model and are based on instrument calibration data. Since the size range of the SMPS was limited to 6−190 nm, we fitted the SMPS measurement data with a product of the lognormal distribution and the size-dependent penetration function. The fits were weighted by the inverse squares of the standard deviations of the average PSD data. The data fitting provided the number-based geometric mean diameter (GMD) and the geometric standard deviation (GSD) at the engine exit plane. Due to low penetration of particles <10 nm, the measurement uncertainties of these particles can be very high, and thus a lower limit of 10 nm at the engine exit plane is used in the system loss correction.[43] The number-based nvPM correction factors were in the range of 2−6 (i.e., 2−6-fold losses) and the mass-based nvPM correction factors were in the range of 1.09−1.54 (i.e., 9−54% loss). These loss-correction factors are in line with previous works that calculated size-dependent losses in standardized nvPM sampling and measurement systems using PSD data for various gas turbine engines.[36,44,45] The penetration functions and details of the system loss-correction calculation are shown in S1 of the SI.

Emission Indices. The EI_{mass} and EI_{num} were calculated using the complete EI formula, taking into account the carbon monoxide (CO) and hydrocarbon (HC) gas concentrations in the exhaust and the different atomic hydrogen/carbon (H/C) ratios of the two fuels.[29] The emission indices are reported at standard temperature and pressure (STP; 0 °C and 101.325 kPa). We also calculated the SMPS number- and mass-based EIs for evaluating the relative reduction of nvPM emissions as a function of engine thrust and fuel hydrogen content. The SMPS-based concentrations were calculated by summing the number and mass concentrations in the size bins (6−190 nm). The mass concentrations were calculated by assuming a constant average particle density of 1 g/cm^3.[46] The total standard uncertainties (95% confidence) in the EIs were estimated using the root-sum-square method to propagate the uncertainties in the parameters measured as described in the SAE ARP6320.[29] Using the typical values for systematic standard uncertainty (10%) and random standard uncertainty (3%) for nvPM mass and number measurement, the total standard uncertainty was 12% for EI_{mass} and 13% for EI_{num}. These uncertainties include assumed 2% total uncertainty for the thermophoretic loss-correction factor k_{thermo}. This low uncertainty agrees with recent experiments that found negligible differences between the standardized k_{thermo} correction model and the experimental data.[35] The uncertainties in the particle loss-corrected EIs were calculated by propagating the total uncertainty in the EIs with the loss-correction uncertainties. The estimated uncertainties in the loss-corrected EIs were 22% for EI_{mass} and 26% for EI_{num}. Previously, uncertainties between 20 and 38% were reported for nvPM EIs without and with loss correction.[25,26,36,44]

LTO Cycle Emissions. The average EIs and fuel flow at the standard sea level (15 °C, 101.325 kPa) were used to calculate emissions from the ICAO LTO cycle. The LTO cycle simulates emissions from airport operations < 915 m (3000

https://doi.org/10.1021/acs.est.1c04744
Environ. Sci. Technol. 2021, 55, 14576−14585

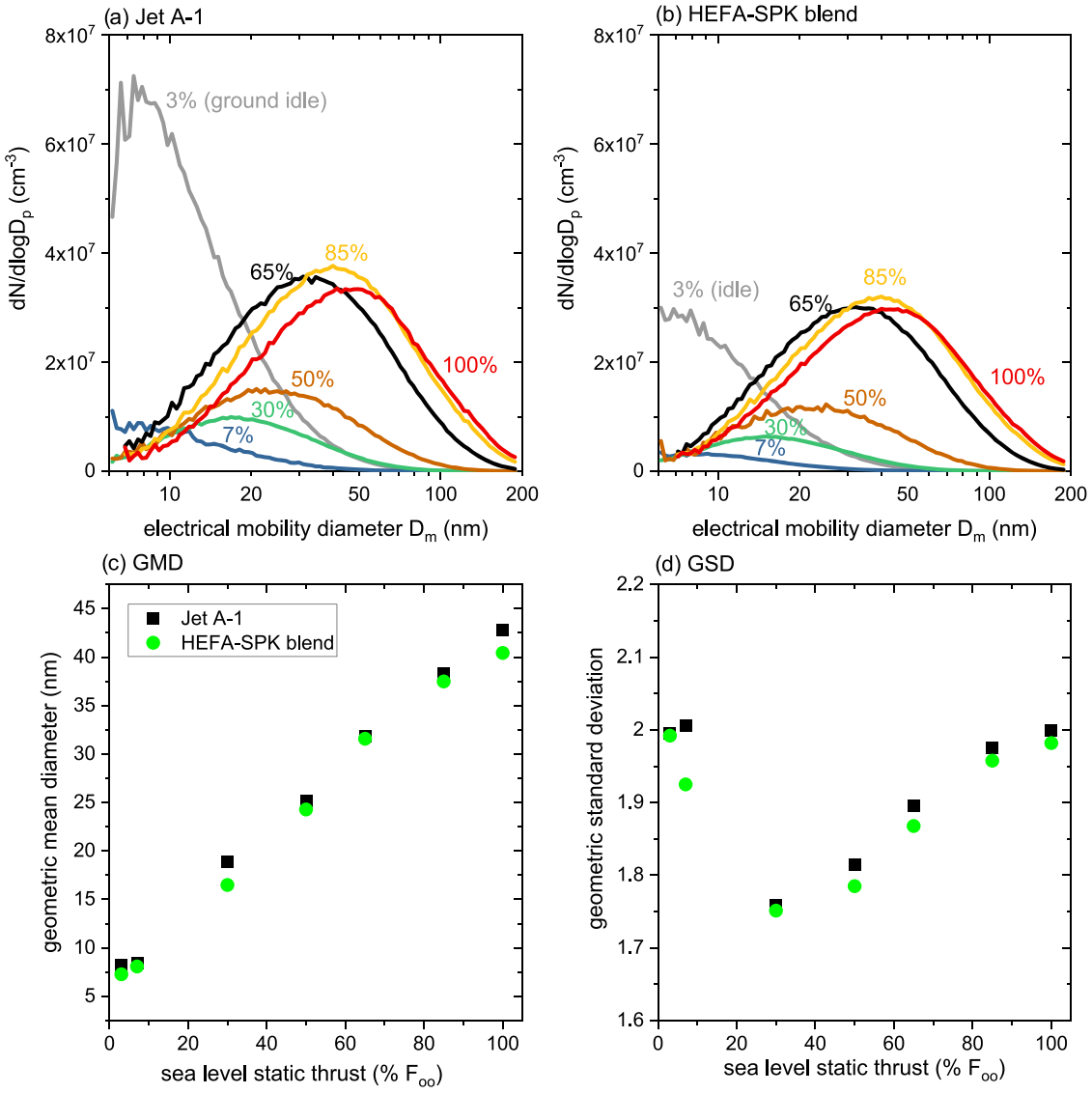

Figure 1. Average particle size distributions at the engine exit plane (corrected for dilution and particle losses in the sampling and measurement system) at different thrust levels ranging from ground idle to take-off obtained with Jet A-1 (a) and the 32% HEFA-SPK blend (b). Panels (c) and (d) show the GMD and GSD of lognormal distributions at the engine exit plane obtained by fitting the SMPS measurement data with the product of the lognormal distribution and the sampling system penetration function ($R^2 > 0.985$; SI). The highest reduction in particle concentration can be seen at low thrust. A small reduction in GMD and GSD was observed with the HEFA-SPK blend compared to Jet A-1 fuel.

ft) above ground level. The EI in each mode is multiplied by fuel flow and the mode duration (26, 4, 2.2, and 0.7 min for taxi, approach, climb-out, and take-off, respectively).

RESULTS AND DISCUSSION

Particle Size Distribution Properties. The particle size distribution properties varied with the engine thrust (Figure 1). At ground idle, the PSD had a GMD of ~8 nm and GSD of ~2 with both fuels. The PSD at ground idle with regular Jet A-1 had the highest number concentration for all test points investigated (Figure 1a). When the thrust increased slightly to 7% F_{oo}, the particle number concentration decreased by an order of magnitude. With further increase in thrust, the number concentration increased and reached a plateau between 65% and 100% F_{oo}. The GMD increased linearly with thrust and the GSD increased from 30% thrust to take-off (Figure 1c,d). Although the number concentration was similar at the three highest power settings, due to the broadening of the PSD and increasing GMD, the mass concentration increased with thrust. The PSD characteristics are in line with previous measurements of the same engine type.[25,26,36] Note that some previous studies report PSD data at the instrument, i.e., without particle loss correction.[25,26] Due to losses, size distributions at the instrument have larger GMD and lower GSD than at the engine exit plane. The GMD and GSD are in the range commonly found for various types of commercial turbofan engines.[25,26,44,47]

The HEFA-SPK blend reduced particle concentrations in the PSD at all thrust levels (Figure 1a,b). The most notable reduction was observed at ground idle and 7% F_{oo}, where the PSD number concentration was reduced by ~60%, and only a small reduction (10−15%) was observed at high thrust. The HEFA-SPK blend reduced the GMD by up to 2.5 nm and the GSD by up to 0.1 (Figure 1c,d). These findings agree with previous studies conducted at the ground level and cruise with different HEFA-SPK blends, which have demonstrated

https://doi.org/10.1021/acs.est.1c04744
Environ. Sci. Technol. 2021, 55, 14576−14585

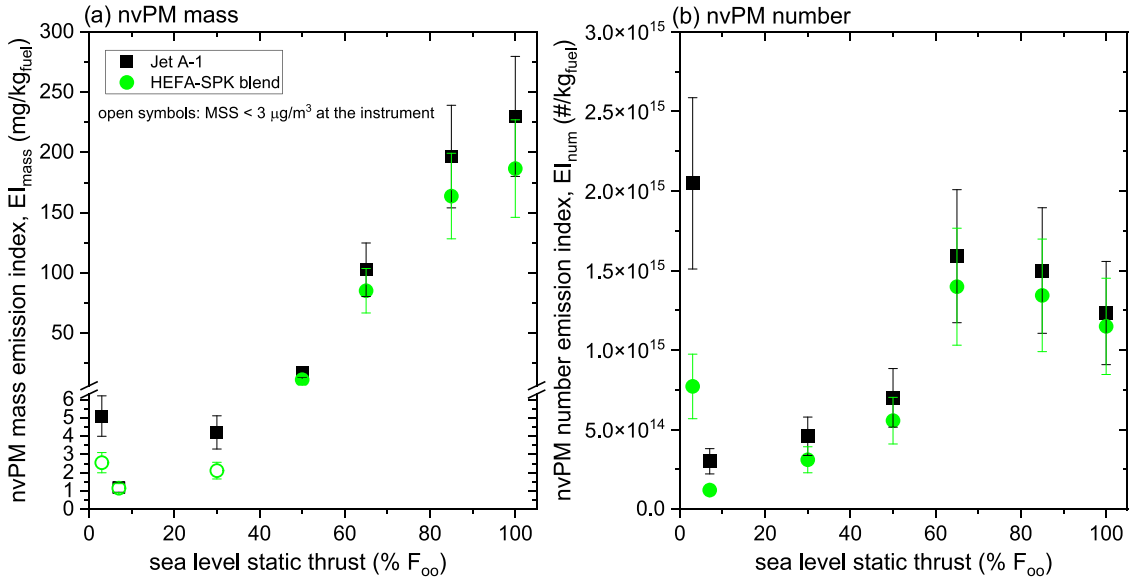

Figure 2. Emission indices of nvPM mass (a) and nvPM number (b) at the engine exit plane (corrected for particle loss in the sampling and measurement system) and STP (0 °C and 101.325 kPa). The open symbols highlight the test points with high nvPM mass measurement uncertainties due to low concentration at the measurement location (<3 $\mu g/m^3$ at ground idle and 30% F_{oo} and <1 $\mu g/m^3$ at 7% F_{oo}). The error bars represent the 2-σ (95% confidence) propagated uncertainties in the loss-corrected EIs (22% for EI_{mass} and 26% for EI_{num}).

relatively small reductions in GMD and GSD for HEFA-SPK blends <50%. A similar reduction of GMD (~3 nm) was reported for an auxiliary power unit (APU) burning HEFA-SPK blends with Jet A-1 in the same range of fuel H/C ratios as investigated here (1.88−1.95).[6] A 50% HEFA blend reduced the GMD produced by a CFM56 engine at cruise by ~4.5 nm.[10] Higher reductions in GMD, by up to 30 nm, have been achieved only with higher blend ratios and pure SPK fuels.[6,12,14,23,34]

Emission Indices of nvPM Mass and Number. The nvPM EI characteristics followed the thrust dependence of the particle size distribution properties. The EI_{mass} had a local maximum at ground idle, then decreased to the minimum at 7% F_{oo}, and subsequently increased steeply with further increase in thrust (Figure 2a). The EI_{num} had a similar trend (Figure 2b). However, the maximum was measured at ground idle with Jet A-1 fuel. At high thrust, the EI_{num} peaked at 65% F_{oo} and decreased with further increase in thrust. The nvPM emission characteristics compare well with the studies of the same engine family using Jet A-1 fuel. However, the maximum EI_{mass} found here was higher than that reported previously.[25,26,36] The maximum EI_{mass} was more than a factor of two higher than that reported for the same engine type with an improved combustor (10% lower certified smoke number) burning regular Jet A-1 tested in the same facility.[36] In addition to the combustor differences, the higher nvPM emissions can be attributed to ambient temperature effects, engine deterioration, and different exhaust sampling probes. First, the data reported by Durdina et al.[36] were obtained at ambient temperatures between 15 and 34 °C (compared to 7.5−12.5 °C here). An engine with maximum nvPM mass emissions at full thrust produces lower EI_{mass} at the T_3 corresponding to take-off at the standard sea level (ISA, 15 °C, 101.325 kPa) in warm conditions than in cold conditions. The combustor inlet pressure p_3 and the combustor discharge fuel−air ratio FAR_4 at a given T_3 decrease with increasing ambient temperature. The nvPM mass reduction correlates with the decrease in p_3 and FAR_4.[17,48] Second, the engines tested in the previous study had a lower number of flight cycles with emission performance comparable to a new engine. The effects of engine aging and ambient conditions on nvPM EIs have been investigated, but as of yet, no parametrizations are available. Lastly, although optimized for carbon balance, the single-orifice exhaust sampling probe used here may not capture the spatial variability of nvPM at the engine exit plane in comparison to the multiorifice probe used previously.[36] For the engine type tested, the spatial variability of EI_{mass} and EI_{num} decreased with increasing thrust. At high thrust, EI_{mass} and EI_{num} determined using the multiorifice and single-orifice probe have been found to be within ~20%.[26] However, these differences do not affect the relative nvPM emissions reductions due to fuel composition effects investigated here.

The EI_{mass} and E_{Inum} decreased with the HEFA-SPK blend at each test point except for the EI_{mass} at 7% F_{oo} due to high measurement uncertainties at low nvPM mass concentrations (Figure 2a). As highlighted by the open symbols, the nvPM mass measured at and below 30% F_{oo} with the HEFA-SPK blend and at 7% F_{oo} with Jet A-1 were below 3 $\mu g/m^3$ at the measurement location. The lowest concentrations detected at 7% F_{oo} were below the specified limit of detection of the MSS (LOD; 1 $\mu g/m^3$). The reductions of nvPM emissions can be attributed to the higher hydrogen mass content (+0.48%) and lower total aromatics (−6.8%) and naphthalenes (−0.26%) of the HEFA-SPK blend compared to Jet A-1, which is consistent with previous research.[5−8,11,21,23,33,45] Also, the HEFA-SPK blend had a higher smoke point, which has been historically used for correlating gas turbine smoke emissions with fuels containing different amounts of total aromatics, naphthalenes, and hydrogen (Table 1).[18]

Prediction of Fuel Composition Effects on nvPM Emissions. This work has provided essential data for developing the first standardized model of fuel composition effects used for emission certification to the new CAEP/11 nvPM standard. Studies have shown that nvPM emissions of various gas turbine engine types correlate with fuel hydrogen content regardless of the naphthalene and aromatic con-

https://doi.org/10.1021/acs.est.1c04744
Environ. Sci. Technol. 2021, 55, 14576−14585

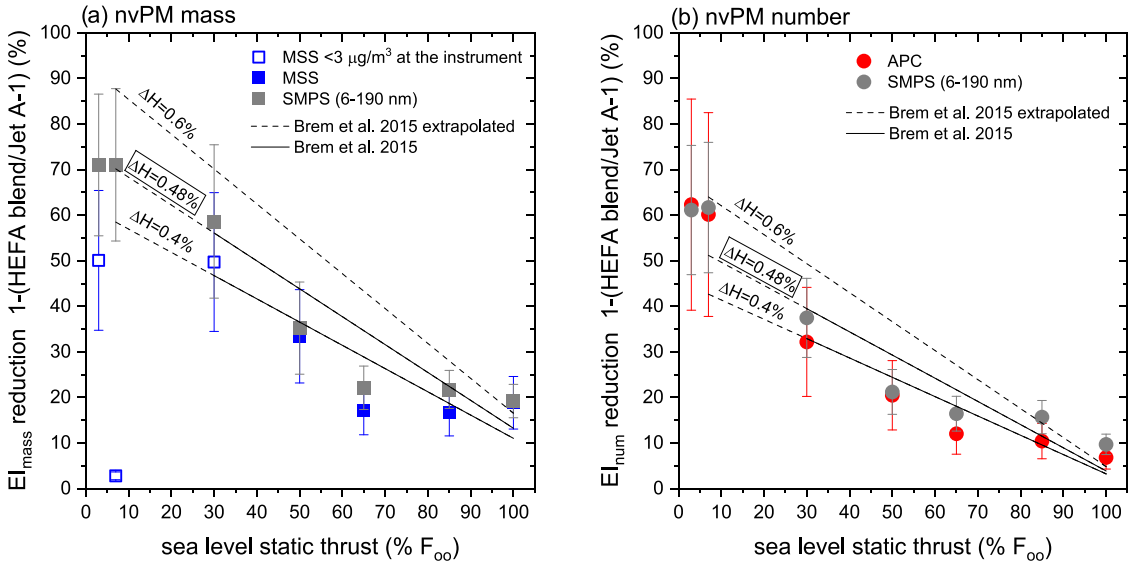

Figure 3. Reduction of the emission indices of nvPM mass (a) and nvPM number (b) with the 32% HEFA-SPK blend with respect to Jet A-1 at the engine exit plane (corrected for particle loss in the sampling and measurement system). The error bars represent the propagated 2σ (95% confidence) combined uncertainties in the loss-corrected EIs. The lines represent the predictive model for EI_{mass} and EI_{num} reduction from Brem et al.,[21] a function of % F_{oo} and the difference in the fuel hydrogen content between the two fuels investigated (ΔH). ΔH of 0.48% (framed) corresponds to the value in this study.

tent.[6,21,23,45] The standardized model utilizes fuel hydrogen content (ΔH, difference between the hydrogen content in the fuel used and the reference value of 13.8%) and engine thrust (% F_{oo}).[28,30] The fuel composition effects are thrust-dependent. Thus, the trends of the EI_{mass} and EI_{num} reductions with thrust (% F_{oo}) for different ΔH must be well known. In the context of our study, ΔH is the difference in the hydrogen content between the two fuels investigated (0.48% using the NMR-determined values in Table 1).

The EI_{mass} and EI_{num} reductions depended strongly on engine thrust setting, with the highest reductions found at low thrust (Figure 3). As described above, the low thrust settings produced extremely low nvPM mass concentrations (<3 $\mu g/m^3$ at the instrument). Thus, EI_{mass} reductions using the MSS data at the lowest three thrust levels have very high uncertainties (open squares in Figure 3a). At such low nvPM mass concentrations, the more sensitive particle size distribution measurement is a useful surrogate for this analysis (gray squares and circles). The SMPS-based EI_{mass} reduction was ~70% at ground idle and 7% F_{oo}. At thrust levels > 30% F_{oo}, EI_{mass} reductions determined using the MSS and SMPS agreed well and decreased steeply with an increase in thrust, reaching ~20% at 65% F_{oo}. With a further increase in thrust, the EI_{mass} reduction remained constant. At high thrust, the upper limit of the SMPS scans (190 nm) cuts off up to ~30% of the particle volume distribution, which may lead to potential discrepancies in the EI_{mass} reduction predicted with the SMPS compared to the MSS. Further sources of potential discrepancy between the MSS and SMPS-derived EI_{mass} reductions are changing PM chemical composition (EC/total carbon (TC) ratio), MAC, and effective density with fuel composition. The EC/TC ratio and MAC may affect the MSS measurement, whereas the effective density affects the SMPS-derived EI_{mass}. All of these parameters remained the same as a function of thrust using the HEFA-SPK blend compared with Jet A-1.[37,49]

The thrust dependence of the EI_{num} reduction was similar to the EI_{mass} but with lower values at each thrust level (Figure 3b). At idle and 7% F_{oo}, the EI_{num} reduction was ~60%, identical for the APC and SMPS. The EI_{num} reduction decreased steeply with an increased thrust to ~12% at 65% F_{oo}. In contrast to EI_{mass} reduction, the EI_{num} reduction decreased slightly with further increase in thrust, reaching ~7% at take-off. The consistently lower EI_{num} reduction can be explained by the effect of the decreasing GMD and GSD on the particle mass distribution (third power of the particle diameter). This observation is consistent with previous studies.[8,21]

The thrust dependence of fuel composition effects qualitatively agrees with previous works, which found the highest PM and nvPM emissions reductions at low power. This effect has been seen across different jet engine technologies and sizes.[5,7,8,11,16,33,50] The interdependencies between the local equivalence ratio governing the soot formation and fuel composition for the engine type investigated have been described in detail by Brem et al.[21] At high engine power, local equivalence ratios are highest and soot is formed mainly by fragmentation and polymerization reactions in fuel-rich flame zones. With decreasing thrust, the local equivalence ratio decreases, mixing improves, the residence time in the primary zone increases, and the soot formation favors the faster condensation reactions with aromatics.[7] A direct comparison with most of the previous emission measurements using alternative fuel blends is difficult as they used various sampling and measurement methodologies not compliant with the ICAO nvPM standard. However, we can compare the results of this study with the model developed by Brem et al.[21] who employed the same standardized sampling and measurement system and the same engine type.

The comparison with the fuel composition effects model of Brem et al. shows notable differences in the thrust-dependent reductions (Figure 3). The model predicts a linear relationship between the EI reduction and % F_{oo} for a given ΔH. The model was developed from emission tests using Jet A-1 fuel doped with aromatic solvents in the thrust range 30−100% F_{oo}

https://doi.org/10.1021/acs.est.1c04744
Environ. Sci. Technol. 2021, 55, 14576−14585

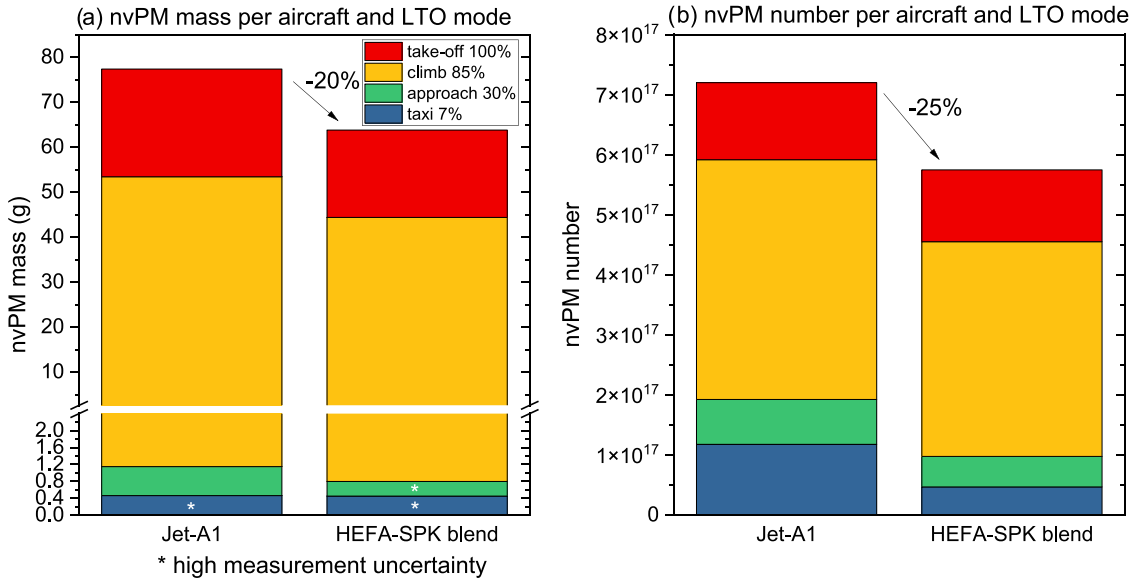

Figure 4. Calculated emissions from the certification landing and take-off cycle (LTO) for nvPM mass (a) and nvPM number (b) per aircraft (two engines operating at the same thrust). The different colors represent the four LTO cycle modes. The emissions in each mode are calculated by multiplying the EIs by fuel flow and the mode duration. The overall reduction is moderate because the LTO cycle emissions of this engine are dominated by the high thrust modes in which the nvPM emissions reductions were the lowest. The most significant reduction was observed for the nvPM number emissions in the taxi mode.

and ΔH < 0.55%. The solid lines in Figure 3 represent the applicability range of the model, whereas the dashed lines are extrapolations of the thrust range and ΔH. For illustration, we plot the predicted reductions for ΔH = 0.4%, 0.48% (ΔH in this study), and 0.6%. In agreement with the model, the EI_{mass} reductions were higher than EI_{num} reductions. The extrapolations below 30% F_{oo} predict the reduction at the lowest certified thrust level (taxi, 7% F_{oo}) within 10%. However, the model does not capture the nonlinear thrust dependence with nearly constant EI_{mass} and EI_{num} reductions at the high thrust reported here. The different thrust dependence of the fuel composition effects may be due to a deteriorated emission performance of the engine tested. The engine accumulated three times higher number of flight cycles and hours than in the previous study. Also, the engine tested by Brem et al. had an improved combustor. Using a CFM56-7B engine with the same combustor as used in this study, Lobo et al.[33] reported similar nonlinear thrust-dependent reductions of EI_{mass} and EI_{num} (calculated from particle size distributions) for various SAF/Jet A-1 blends. With each blend, the % reductions in EI_{mass} and EI_{num} decreased with increasing thrust up to 85% F_{oo} and no further decrease was observed at 100% F_{oo}.

This comparison emphasizes the high uncertainties in predicting fuel composition effects on nvPM emissions with published data. Future works should provide further evidence for the applicability of a fuel composition correction based on fuel hydrogen content and engine thrust using different SAF blends and the ICAO Annex 16 sampling and measurement methodology. The tests should be performed on engines with various combustor types, thrust ratings, and overall pressure ratios. Accurate predictions of the fuel composition effects on nvPM emissions become increasingly important for the emission certification and predicting the impact of widespread adoption of SAF on climate and local air quality.

Local Air Quality Impacts. This work provides evidence of the benefits of SAF blends for airport air quality. The 32% HEFA-SPK blend reduced the nvPM mass emissions from the standard LTO cycle by ~20% and the nvPM number emissions by ~25% (Figure 4, no error bars shown for clarity). Although we showed in Figure 3 that the EI_{mass} reductions were higher than the EI_{num} reductions at each thrust level, the nvPM mass contribution to the LTO emissions from the low thrust modes (where the reductions are highest) was only ~1%. In contrast, the nvPM number emissions from the taxi and approach modes with Jet A-1 constituted ~25% of the LTO nvPM number, leading to an overall higher reduction for the nvPM number. The overall reductions were modest because the LTO emissions were dominated by climb (85% F_{oo}) for both nvPM mass and nvPM number. We expect similar potential reductions of the LTO nvPM emissions from the current commercial fleet dominated by engines with maximum nvPM emissions at high thrust.

The relatively high reductions of nvPM number found at low thrust are most significant for the air quality and health effects at airports and surrounding communities. Recent models predict that over 80% of the LTO nvPM number at a large airport is emitted during taxi and approach.[51]

However, the real-world contribution of low thrust operations may be even higher because of ground idle emissions (<7% F_{oo}). As shown above, the EI_{num} at ground idle was an order of magnitude higher than at 7% F_{oo}. Estimating real-world ground idle emissions is a point of controversy as it is not a certification test point and it is set automatically by the engine control unit. Moreover, in real-world operations, bleed air extraction and additional loads affect the fuel−air ratio. Thus, the real-world ground idle emissions may differ from the test cell results.[52] Nevertheless, we expect the relative nvPM emissions reductions found here at ground idle to apply for on-wing operations. Future work should further investigate the reductions of nvPM and volatile PM emissions at low power from on-wing tests at different bleed air extraction levels, auxiliary loads, and ambient conditions.

https://doi.org/10.1021/acs.est.1c04744
Environ. Sci. Technol. 2021, 55, 14576−14585

■ ASSOCIATED CONTENT

Supporting Information

The Supporting Information is available free of charge at https://pubs.acs.org/doi/10.1021/acs.est.1c04744.

S1: Correction for particle loss in the sampling and measurement system (PDF)

Tables with data (XLSX)

■ AUTHOR INFORMATION

Corresponding Authors

Lukas Durdina − *Advanced Analytical Technologies, Empa, Dübendorf CH-8600, Switzerland;* Present Address: Centre for Aviation, School of Engineering, Zurich University of Applied Sciences, Winterthur, CH-8401, Switzerland; orcid.org/0000-0003-3562-879X; Email: lukas.durdina@zhaw.ch

Benjamin T. Brem − *Advanced Analytical Technologies, Empa, Dübendorf CH-8600, Switzerland;* Present Address: Laboratory for Atmospheric Chemistry, Paul Scherrer Institute, Villigen CH-5232, Switzerland; Email: benjamin.brem@psi.ch

Authors

Miriam Elser − *Advanced Analytical Technologies, Empa, Dübendorf CH-8600, Switzerland;* Present Address: Laboratory for Automotive Powertrain Technologies, Empa, Dübendorf CH-8600, Switzerland.

David Schönenberger − *Advanced Analytical Technologies, Empa, Dübendorf CH-8600, Switzerland;* Present Address: Laboratory for Air Pollution and Environmental Technology, Empa, Dübendorf CH-8600, Switzerland.

Frithjof Siegerist − *SR Technics Switzerland AG, Zurich-Airport CH-8058, Switzerland*

Julien G. Anet − *Centre for Aviation, School of Engineering, Zurich University of Applied Sciences, Winterthur CH-8401, Switzerland*

Complete contact information is available at: https://pubs.acs.org/10.1021/acs.est.1c04744

Notes

The authors declare no competing financial interest.

■ ACKNOWLEDGMENTS

The authors are grateful to SR Technics for their support regarding engine lease and the engine and test cell operation. The authors thank Christian Bach and Martin Oertig of Empa for the help with the alternative fuel blend import. The authors thank Dr. Daniel Rentsch and Regula Haag of Empa for the NMR fuel hydrogen content analysis. The authors also thank Dr. Prem Lobo for helpful comments. This work was made possible by funding from the Swiss Federal Office of Civil Aviation (FOCA) through projects EMPAIREX (SFLV 2015-113), AGEAIR (SFLV 2017-030), and AGEAIR 2 (SFLV 2018-048).

■ REFERENCES

(1) ICAO Secretariat *Introduction to the ICAO Basket of Measures to Mitigate Climate Change*, ICAO 2019 Environmental Report, 2019; pp 111−115.

(2) ASTM D7566-20B*Specification for Aviation Turbine Fuel Containing Synthesized Hydrocarbons. D7566-20B*; ASTM International: West Conshohocken, PA.

(3) ASTM D1655-20C*Specification for Aviation Turbine Fuels. D1655-20C*; ASTM International: West Conshohocken.

(4) Staples, M. D.; Malina, R.; Suresh, P.; Hileman, J. I.; Barrett, S. R. Aviation CO2 emissions reductions from the use of alternative jet fuels. *Energy Policy* **2018**, *114*, 342−354.

(5) Beyersdorf, A. J.; Timko, M. T.; Ziemba, L. D.; Bulzan, D.; Corporan, E.; Herndon, S. C.; Howard, R.; Miake-Lye, R.; Thornhill, K. L.; Winstead, E.; Wey, C.; Yu, Z.; Anderson, B. E. Reductions in aircraft particulate emissions due to the use of Fischer−Tropsch fuels. *Atmos. Chem. Phys.* **2014**, *14*, 11−23.

(6) Christie, S.; Lobo, P.; Lee, D.; Raper, D. Gas Turbine Engine Nonvolatile Particulate Matter Mass Emissions: Correlation with Smoke Number for Conventional and Alternative Fuel Blends. *Environ. Sci. Technol.* **2017**, *51*, 988−996.

(7) Corporan, E.; DeWitt, M. J.; Belovich, V.; Pawlik, R.; Lynch, A. C.; Gord, J. R.; Meyer, T. R. Emissions Characteristics of a Turbine Engine and Research Combustor Burning a Fischer−Tropsch Jet Fuel. *Energy Fuels* **2007**, *21*, 2615−2626.

(8) Lobo, P.; Condevaux, J.; Yu, Z.; Kuhlmann, J.; Hagen, D. E.; Miake-Lye, R. C.; Whitefield, P. D.; Raper, D. W. Demonstration of a Regulatory Method for Aircraft Engine Nonvolatile PM Emissions Measurements with Conventional and Isoparaffinic Kerosene fuels. *Energy Fuels* **2016**, *30*, 7770−7777.

(9) Lobo, P.; Rye, L.; Williams, P. I.; Christie, S.; Uryga-Bugajska, I.; Wilson, C. W.; Hagen, D. E.; Whitefield, P. D.; Blakey, S.; Coe, H.; Raper, D.; Pourkashanian, M. Impact of alternative fuels on emissions characteristics of a gas turbine engine - part 1: gaseous and particulate matter emissions. *Environ. Sci. Technol.* **2012**, *46*, 10805−10811.

(10) Moore, R. H.; Thornhill, K. L.; Weinzierl, B.; Sauer, D.; D'Ascoli, E.; Kim, J.; Lichtenstern, M.; Scheibe, M.; Beaton, B.; Beyersdorf, A. J.; Barrick, J.; Bulzan, D.; Corr, C. A.; Crosbie, E.; Jurkat, T.; Martin, R.; Riddick, D.; Shook, M.; Slover, G.; Voigt, C.; White, R.; Winstead, E.; Yasky, R.; Ziemba, L. D.; Brown, A.; Schlager, H.; Anderson, B. E. Biofuel blending reduces particle emissions from aircraft engines at cruise conditions. *Nature* **2017**, *543*, 411−415.

(11) Schripp, T.; Anderson, B.; Crosbie, E. C.; Moore, R. H.; Herrmann, F.; Oßwald, P.; Wahl, C.; Kapernaum, M.; Köhler, M.; Le Clercq, P.; Rauch, B.; Eichler, P.; Mikoviny, T.; Wishaler, A. Impact of Alternative Jet Fuels on Engine Exhaust Composition During the 2015 ECLIF Ground-Based Measurements Campaign. *Environ. Sci. Technol.* **2018**, *52*, 4969−4978.

(12) Timko, M. T.; Yu, Z.; Onasch, T. B.; Wong, H.-W.; Miake-Lye, R. C.; Beyersdorf, A. J.; Anderson, B. E.; Thornhill, K. L.; Winstead, E. L.; Corporan, E.; DeWitt, M. J.; Klingshirn, C. D.; Wey, C.; Tacina, K.; Liscinsky, D. S.; Howard, R.; Bharagava, A. Particulate Emissions of Gas Turbine Engine Combustion of a Fischer−Tropsch Synthetic Fuel. *Energy Fuels* **2010**, *24*, 5883−5896.

(13) Tran, S.; Brown, A.; Olfert, J. S. Comparison of Particle Number Emissions from In-Flight Aircraft Fueled with Jet A1, JP-5 and an Alcohol-to-Jet Fuel Blend. *Energy Fuels* **2020**, *34*, 7218−7222.

(14) Kinsey, J. S.; Timko, M. T.; Herndon, S. C.; Wood, E. C.; Yu, Z.; Miake-Lye, R. C.; Lobo, P.; Whitefield, P.; Hagen, D.; Wey, C.; Anderson, B. E.; Beyersdorf, A. J.; Hudgins, C. H.; Thornhill, K. L.; Winstead, E.; Howard, R.; Bulzan, D. U.; Tacina, K. B.; Knighton, W. B. Determination of the emissions from an aircraft auxiliary power unit (APU) during the Alternative Aviation Fuel Experiment (AAFEX). *J. Air Waste Manage. Assoc.* **2012**, *62*, 420−430.

(15) Voigt, C.; Kleine, J.; Sauer, D.; Moore, R. H.; Bräuer, T.; Le Clercq, P.; Kaufmann, S.; Scheibe, M.; Jurkat-Witschas, T.; Aigner, M.; Bauder, U.; Boose, Y.; Borrmann, S.; Crosbie, E.; Diskin, S. G.; DiGangi, J.; Hahn, V.; Heckl, C.; Huber, F.; Nowak, J. B.; Rapp, M.; Rauch, B.; Robinson, C.; Schripp, T.; Shook, M.; Winstead, E.; Ziemba, L.; Schlager, H.; Anderson, B. E. Cleaner burning aviation fuels can reduce contrail cloudiness. *Commun. Earth Environ.* **2021**, *2*, 1−10.

(16) Moore, R. H.; Shook, M.; Beyersdorf, A.; Corr, C.; Herndon, S.; Knighton, W. B.; Miake-Lye, R.; Thornhill, K. L.; Winstead, E. L.; Yu, Z.; Ziemba, L. D.; Anderson, B. E. Influence of Jet Fuel

Composition on Aircraft Engine Emissions: A Synthesis of Aerosol Emissions Data from the NASA APEX, AAFEX, and ACCESS Missions. *Energy Fuels* **2015**, *29*, 2591−2600.
(17) Lefebvre, A. H.; Ballal, D. R. Emissions. In *Gas Turbine Combustion: Alternative Fuels and Emissions*, 3rd ed.; Taylor & Francis: Boca Raton, 2010; Chapter 9, pp 359−441.
(18) Chin, J. S.; Lefebvre, A. H. Influence of Fuel Chemical Properties on Soot Emissions from Gas Turbine Combustors. *Combust. Sci. Technol.* **1990**, *73*, 479−486.
(19) Bowden, T. T.; Pearson, J. H.; Wetton, R. J. The Influence of Fuel Hydrogen Content Upon Soot Formation in a Model Gas Turbine Combustor. *J. Eng. Gas Turbines Power* **1984**, *106*, 789−794.
(20) Masters, A.; Mosier, S. A.; Nowack, C. J. Fuel Property Effects on USN Gas Turbine Combustors. In *Assessment of Alternative Aircraft Fuels, Proceedings of a Conference held at NASA Lewis Research Center*, Cleveland, Ohio, 1983; pp 63−71.
(21) Brem, B. T.; Durdina, L.; Siegerist, F.; Beyerle, P.; Bruderer, K.; Rindlisbacher, T.; Rocci-Denis, S.; Andac, M. G.; Zelina, J.; Penanhoat, O.; Wang, J. Effects of Fuel Aromatic Content on Nonvolatile Particulate Emissions of an In-Production Aircraft Gas Turbine. *Environ. Sci. Technol.* **2015**, *49*, 13149−13157.
(22) Abrahamson, J. P.; Zelina, J.; Andac, M. G.; Vander Wal, R. L. Predictive Model Development for Aviation Black Carbon Mass Emissions from Alternative and Conventional Fuels at Ground and Cruise. *Environ. Sci. Technol.* **2016**, *50*, 12048−12055.
(23) Lobo, P.; Christie, S.; Khandelwal, B.; Blakey, S. G.; Raper, D. W. Evaluation of Non-volatile Particulate Matter Emission Characteristics of an Aircraft Auxiliary Power Unit with Varying Alternative Jet Fuel Blend Ratios. *Energy Fuels* **2015**, *29*, 7705−7711.
(24) Jonsdottir, H. R.; Delaval, M.; Leni, Z.; Keller, A.; Brem, B. T.; Siegerist, F.; Schönenberger, D.; Durdina, L.; Elser, M.; Burtscher, H.; Liati, A.; Geiser, M. Non-volatile particle emissions from aircraft turbine engines at ground-idle induce oxidative stress in bronchial cells. *Commun. Biol.* **2019**, *2*, No. 90.
(25) Lobo, P.; Durdina, L.; Smallwood, G. J.; Rindlisbacher, T.; Siegerist, F.; Black, E. A.; Yu, Z.; Mensah, A. A.; Hagen, D. E.; Miake-Lye, R. C.; Thomson, K. A.; Brem, B. T.; Corbin, J. C.; Abegglen, M.; Sierau, B.; Whitefield, P. D.; Wang, J. Measurement of Aircraft Engine Non-Volatile PM Emissions: Results of the Aviation-Particle Regulatory Instrumentation Demonstration Experiment (A-PRIDE) 4 Campaign. *Aerosol Sci. Technol.* **2015**, *49*, 472−484.
(26) Lobo, P.; Durdina, L.; Brem, B. T.; Crayford, A. P.; Johnson, M. P.; Smallwood, G. J.; Siegerist, F.; Williams, P. I.; Black, E. A.; Llamedo, A.; Thomson, K. A.; Trueblood, M. B.; Yu, Z.; Hagen, D. E.; Whitefield, P. D.; Miake-Lye, R. C.; Rindlisbacher, T. Comparison of standardized sampling and measurement reference systems for aircraft engine non-volatile particulate matter emissions. *J. Aerosol Sci.* **2020**, *145*, No. 105557.
(27) Petzold, A.; Marsh, R.; Johnson, M.; Miller, M.; Sevcenco, Y.; Delhaye, D.; Ibrahim, A.; Williams, P.; Bauer, H.; Crayford, A.; Bachalo, W. D.; Raper, D. Evaluation of methods for measuring particulate matter emissions from gas turbines. *Environ. Sci. Technol.* **2011**, *45*, 3562−3568.
(28) Jacob, S. D.; Rindlisbacher, T. *The Landing and Take-Off Particulate Matter Standards for Aircraft Gas Turbine Engines. ICAO 2019 Environmental Report*, 2019; pp 100−105.
(29) Procedure for the Continuous Sampling and Measurement of Non-Volatile Particulate Matter Emissions from Aircraft Turbine Engines; SAE International: 400 Commonwealth Drive, Warrendale, PA.
(30) Annex 16 to the Convention on International Civil Aviation: Environmental Protection, Vol. II − Aircraft Engine Emissions, 4th ed.; ICAO: Montreal, CA, 2017.
(31) Archilla, V.; Hormigo, D.; Sánchez-García, M.; Raper, D. AVIATOR - Assessing aViation emission Impact on local Air quality at airports: TOwards Regulation. In *MATEC Web of Conferences*; EDP Sciences, 2019; p 2023.
(32) Durdina, L.; Durand, E.; Spirig, C.; Edebeli, J.; Anet, J.; Crayford, A. Intercomparison of Two Reference Sampling and Measurement Systems for Aircraft Engine Nonvolatile PM Using a Small-Scale RQL Combustor Rig Burning Conventional and Sustainable Aviation Fuels. In *24th ETH-Conference on Combustion Generated Nanoparticles*, 2021.
(33) Lobo, P.; Hagen, D. E.; Whitefield, P. D. Comparison of PM emissions from a commercial jet engine burning conventional, biomass, and Fischer-Tropsch fuels. *Environ. Sci. Technol.* **2011**, *45*, 10744−10749.
(34) Cain, J.; DeWitt, M. J.; Blunck, D.; Corporan, E.; Striebich, R.; Anneken, D.; Klingshirn, C.; Roquemore, W. M.; Vander Wal, R. Characterization of Gaseous and Particulate Emissions From a Turboshaft Engine Burning Conventional, Alternative, and Surrogate Fuels. *Energy Fuels* **2013**, *27*, 2290−2302.
(35) Durand, E. F.; Crayford, A. P.; Johnson, M. Experimental validation of thermophoretic and bend nanoparticle loss for a regulatory prescribed aircraft nvPM sampling system. *Aerosol Sci. Technol.* **2020**, *54*, 1019−1033.
(36) Durdina, L.; Brem, B. T.; Setyan, A.; Siegerist, F.; Rindlisbacher, T.; Wang, J. Assessment of Particle Pollution from Jetliners: from Smoke Visibility to Nanoparticle Counting. *Environ. Sci. Technol.* **2017**, *51*, 3534−3541.
(37) Elser, M.; Brem, B. T.; Durdina, L.; Schönenberger, D.; Siegerist, F.; Fischer, A.; Wang, J. Chemical composition and radiative properties of nascent particulate matter emitted by an aircraft turbofan burning conventional and alternative fuels. *Atmos. Chem. Phys.* **2019**, *19*, 6809−6820.
(38) ASTM D7171-20, Test Method for Hydrogen Content of Middle Distillate Petroleum Products by Low-Resolution Pulsed Nuclear Magnetic Resonance Spectroscopy; ASTM International: West Conshohocken, PA.
(39) ASTM D5291, Test Methods for Instrumental Determination of Carbon, Hydrogen, and Nitrogen in Petroleum Products and Lubricants; ASTM International: West Conshohocken, PA.
(40) Schindler, W.; Haisch, C.; Beck, H. A.; Niessner, R.; Jacob, E.; Rothe, D. A Photoacoustic Sensor System for Time Resolved Quantification of Diesel Soot Emissions. In *SAE Technical Paper Series*; SAE International: Warrendale, PA, 2004.
(41) Brem, B. T.; Elser, M.; Arndt, M.; Fischer, A.; Durdina, L.; Schönenberger, D. The Optics-Chemistry Link of Dark Matter; Investigating Mass Absorption Cross Sections of Soot Particles from Two Combustion Sources. In *22nd ETH-Conference on Combustion Generated Nanoparticles*, 2018.
(42) Kinsey, J. S.; Giannelli, R.; Howard, R.; Hoffman, B.; Frazee, R.; Aldridge, M.; Leggett, C.; Stevens, K.; Kittelson, D.; Silvis, W.; Stevens, J.; Lobo, P.; Achterberg, S.; Swanson, J.; Thomson, K.; McArthur, T.; Hagen, D.; Trueblood, M.; Wolff, L.; Liscinsky, D.; Arey, R.; Cerully, K.; Miake-Lye, R.; Onasch, T.; Freedman, A.; Bachalo, W.; Payne, G.; Durlicki, M. Assessment of a regulatory measurement system for the determination of the non-volatile particulate matter emissions from commercial aircraft engines. *J. Aerosol Sci.* **2021**, *154*, No. 105734.
(43) Procedure for the Calculation of Non-Volatile Particulate Matter Sampling and Measurement System Losses and System Loss Correction Factors; SAE International: 400 Commonwealth Drive, Warrendale, PA.
(44) Durdina, L.; Brem, B. T.; Schönenberger, D.; Siegerist, F.; Anet, J. G.; Rindlisbacher, T. Nonvolatile Particulate Matter Emissions of a Business Jet Measured at Ground Level and Estimated for Cruising Altitudes. *Environ. Sci. Technol.* **2019**, *53*, 12865−12872.
(45) Durand, E.; Lobo, P.; Crayford, A.; Sevcenco, Y.; Christie, S. Impact of fuel hydrogen content on non-volatile particulate matter emitted from an aircraft auxiliary power unit measured with standardised reference systems. *Fuel* **2021**, *287*, No. 119637.
(46) Durdina, L.; Brem, B. T.; Abegglen, M.; Lobo, P.; Rindlisbacher, T.; Thomson, K. A.; Smallwood, G. J.; Hagen, D. E.; Sierau, B.; Wang, J. Determination of PM mass emissions from an aircraft turbine engine using particle effective density. *Atmos. Environ.* **2014**, *99*, 500−507.

https://doi.org/10.1021/acs.est.1c04744
Environ. Sci. Technol. 2021, 55, 14576−14585

(47) Saffaripour, M.; Thomson, K. A.; Smallwood, G. J.; Lobo, P. A review on the morphological properties of non-volatile particulate matter emissions from aircraft turbine engines. *J. Aerosol Sci.* **2020**, *139*, No. 105467.
(48) Petzold, A.; Döpelheuer, A.; Brock, C. A.; Schröder, F. In situ observations and model calculations of black carbon emission by aircraft at cruise altitude. *J. Geophys. Res.* **1999**, *104*, 22171−22181.
(49) Durdina, L.; Brem, B. T.; Elser, M.; Schönenberger, D.; Anet, J. G. Effective Density of Aircraft Engine PM Revisited: Effects of Engine Thrust, Engine Type, Fuel, and Sample Conditioning. In *European Aerosol Conference*, 2021.
(50) Speth, R. L.; Rojo, C.; Malina, R.; Barrett, S. R. Black carbon emissions reductions from combustion of alternative jet fuels. *Atmos. Environ.* **2015**, *105*, 37−42.
(51) Lorentz, H.; Schmidt, W.; Hellebrandt, P.; Ketzel, M.; Jakobs, H.; Janicke, U. Einfluss eines Großflughafens auf zeitliche und räumliche Verteilungen der Außenluftkonzentrationen von Ultrafeinstaub <100 nm, um die potentielle Belastung in der Nähe zu beschreiben − unter Einbeziehung weiterer Luftschadstoffe (Ruß, Stickoxide und Feinstaub (PM2,5 und PM10)), 2021.
(52) Herndon, S. C.; Wood, E. C.; Frankli, J.; Miake-Lye, R. C.; Knighton, W. B.; Babb, M.; Nakahara, A.; Reynolds, T.; Balakrishnan, H. *Measurement of Gaseous HAP Emissions from Idling Aircraft as a Function of Engine and Ambient Conditions*, ACRP Report 63; Transportation Research Board: Washington, DC, 2012.

https://doi.org/10.1021/acs.est.1c04744
Environ. Sci. Technol. 2021, 55, 14576−14585